

Measurement report: Source characteristics of water-soluble organic carbon in PM_{2.5} at two sites in Japan, as assessed by long-term observation and stable carbon isotope ratio

Nana Suto¹, Hiroto Kawashima²

5 ¹ Energy and Environment Research Division, Japan Automobile Research Institute, Tsukuba, 3050822, Japan

² Faculty of Systems Science and Technology, Akita Prefectural University, Yurihonjo, 0150055, Japan

Correspondence to: Nana Suto (nsuto@jari.or.jp) and Hiroto Kawashima (kawashima@akita-pu.ac.jp)

Abstract. The sources and seasonal trends of water-soluble organic carbon (WSOC) in carbonaceous aerosols are of significant interest. From July 2017 to July 2019, we collected samples of PM_{2.5} (particulate matter, aerodynamic diameter < 2.5 μm)

10 from one suburban and one rural site in Japan. The average $\delta^{13}\text{C}_{\text{WSOC}}$ was $-25.2 \pm 1.1\text{‰}$ and $-24.6 \pm 2.4\text{‰}$ at the suburban site and rural site, respectively. At the suburban site, the $\delta^{13}\text{C}_{\text{WSOC}}$ was consistent with the $\delta^{13}\text{C}$ of C3 plant burning, and a high correlation was found between WSOC concentration and non-sea-salt potassium concentration. These results suggested that the main source of WSOC was biomass burning of rice straw. At the rural site, the average $\delta^{13}\text{C}_{\text{WSOC}}$ was significantly heavier from autumn to spring ($-23.9 \pm 2.1\text{‰}$) than in summer ($-27.4 \pm 0.7\text{‰}$) ($p < 0.01$). The $\delta^{13}\text{C}_{\text{WSOC}}$ from autumn to spring were 15 a result mainly of biomass burning of rice straw, whereas the $\delta^{13}\text{C}_{\text{WSOC}}$ in summer was a result mainly of the formation of secondary organic aerosols from biogenic volatile organic compounds. In particular, the reason for the heaviest $\delta^{13}\text{C}_{\text{WSOC}}$ ($-21.3 \pm 1.9\text{‰}$) from February to April 2019 might be affected by long-range transport of C4 plant burning such as corn from overseas. Thus, our $\delta^{13}\text{C}_{\text{WSOC}}$ approach was useful to elucidate the sources and atmospheric processes that contribute to seasonal variations of WSOC concentrations.

20 1 Introduction

Particulate matter (PM) has deleterious effects on human health and contributes to climate change (Pope et al., 1995; Lohmann and Feichter, 2005). A major component of PM_{2.5} (particulate matter, aerodynamic diameter < 2.5 μm) is carbonaceous aerosol, which comprises organic carbon (OC) and elemental carbon (EC) (Chow et al., 1993; Malm et al., 2004; Pöschl, 2005). The OC in carbonaceous aerosol can be further classified water-insoluble organic carbon (WIOC) and water-25 soluble organic carbon (WSOC) (Sullivan and Weber, 2006). WIOC is produced mainly by the combustion of fossil fuels and contains compounds such as alkanes (Pöschl, 2005). WSOC is emitted primarily from combustion processes, industrial process, and natural sources. It can also be formed through secondary processes such as homogeneous gas-phase or heterogeneous aerosol-phase oxidation (Claeys et al., 2004; Koch et al., 2007; Schichtel et al., 2008). WSOC accounts for 20%–80% of the total OC in carbonaceous aerosol depending on the location and season (Decesari et al., 2001; Sullivan et al., 2004; Du et al.,

30 2014; Duarte et al., 2015; Zhang et al., 2019). In addition, an average of 74% of all WSOC is contained in fine particles (Yu et al., 2004). WSOC is hygroscopic and therefore it enhances the capability of aerosols to act as cloud condensation nuclei, which affects climate change (Padró et al., 2010; Asa-Awuku et al., 2011). Therefore, source contributions of WSOC have been of significant interest for decades. A common approach for estimating the source contributions of WSOC is the use of a positive matrix factorization (PMF) model. Using this approach, the annual contributions of biomass burning and secondary 35 processes to WSOC in Beijing, China, were estimated to be 40% and 54%, respectively (Du et al., 2014). Similarly, in Helsinki, Finland, the contribution of secondary organic aerosol (SOA) to WSOC is reported to be high in summer (78%) but low in winter (28%) (Saarikoski et al., 2008). WSOC is known to contain various oxygenated compounds, including dicarboxylic acids, ketocarboxylic acids, aliphatic aldehydes, alcohols, saccharides, saccharide anhydrides, aromatic acids, phenols, amines, amino acids, organic nitrates, and organic sulfates (Duarte et al., 2007; Pietrogrande et al., 2013; Timonen et al., 2013; Chalbot 40 et al., 2014; Duarte et al., 2015). However, the precise molecular composition of WSOC is poorly understood because of the large number of compounds involved and the difficulties involved in identifying the individual components.

The stable carbon isotope ratio ($\delta^{13}\text{C}$) of carbonaceous aerosols can provide useful information about a sample of PM (e.g., Widory et al., 2004; Fisseha et al., 2009; Cao et al., 2011; Gensch et al., 2014). Since EC is unreactive, it is possible to identify the source from $\delta^{13}\text{C}_{\text{EC}}$ in their aerosols directly (e.g., Kawashima and Haneishi, 2012; Zhao et al., 2018). In contrast, 45 OC reacts in the atmosphere, so their $\delta^{13}\text{C}_{\text{OC}}$ provide information not only on the source of the PM but also on any atmospheric processing it has undergone (e.g., Cao et al., 2011; Ni et al., 2018). The measurement of $\delta^{13}\text{C}_{\text{WSOC}}$ in PM has been actively carried out in recent years (e.g., Kirillova et al., 2010; Kirillova et al., 2013b; Suto and Kawashima, 2018; Zhang et al., 2019). The analysis of $\delta^{13}\text{C}_{\text{WSOC}}$ in ambient aerosol has been performed by wet oxidation method using GasBench/isotope ratio mass 50 spectrometry (IRMS) (Fisseha et al., 2006) and combustion method using elemental analyzer/IRMS (EA/IRMS) (Kirillova et al., 2010). In the past few years, a highly sensitive analytical methods for $\delta^{13}\text{C}_{\text{WSOC}}$ based on wet oxidation using liquid chromatography/IRMS (LC/IRMS) (Suto and Kawashima, 2018) and GasBench/IRMS (Zhang et al., 2019), and total organic carbon analyzer/IRMS (Han et al., 2020) have been developed. The combustion method is the most widely used approach today. The $\delta^{13}\text{C}_{\text{WSOC}}$ of various particle size collected has been reported at various times in East Asia (Miyazaki et al., 2012; Kirillova et al., 2014a; Pavuluri and Kawamura, 2017; Yan et al., 2017; Suto and Kawashima, 2018; Zhang et al., 2019; Han 55 et al., 2020), South Asia (Kirillova et al., 2013b; Bosch et al., 2014; Kirillova et al., 2014b; Dasari et al., 2019), Europe (Fisseha et al., 2006; Fisseha et al., 2009; Kirillova et al., 2010), and the United States (Wozniak et al., 2012a; Wozniak et al., 2012b) (Table S1 in the Supplement).

For example, the $\delta^{13}\text{C}$ of total carbon ($\delta^{13}\text{C}_{\text{TC}}$) and $\delta^{13}\text{C}_{\text{WSOC}}$ of total suspended particles (TSP) was observed from September 2009 to October 2010 in Hokkaido, Japan (Pavuluri and Kawamura, 2017). Both $\delta^{13}\text{C}_{\text{TC}}$ and $\delta^{13}\text{C}_{\text{WSOC}}$ were heavier 60 in winter than in summer, demonstrating seasonal variation. The authors concluded that the reason why $\delta^{13}\text{C}_{\text{WSOC}}$ was heavy in winter was because of the greater release of ^{13}C by fossil fuel combustion and biomass burning. Similarly, Kirillova et al. (2013a) collected TSP samples from January 2008 to April 2009 in Sinhagad, India, and Hanimaadhoo Island, Maldives. The average $\delta^{13}\text{C}_{\text{WSOC}}$ was $-20.4 \pm 0.5\text{‰}$ in Sinhagad and $-18.4 \pm 0.5\text{‰}$ in Hanimaadhoo Island, which are heavier than values

reported in other studies. In addition, aerosols reaching Hanimaadhoo Island after long-range, over-ocean transport were
65 enriched by 3‰–4‰ in $\delta^{13}\text{C}_{\text{WSOC}}$ relative to the aerosols collected in Sinhagad. Based on these findings, Kirillova et al.
reported for the first time that this enrichment of $\delta^{13}\text{C}$ was an effect related to the aging of OC during long-range transport of
aerosol. Recent study reported that the enrichment of $\delta^{13}\text{C}_{\text{WSOC}}$ between source site (Delhi, India) and receptor site
(Hanimaadhoo Island, Maldives) is caused by aging effect during long-range transport (Dasari et al., 2019).

The combustion method, which is widely used at present, requires more pretreatment time because samples of PM
70 are extracted, dehydrated with a freeze drier, dried, and then measured by EA/IRMS. The wet oxidation/IRMS method
described above do not require a drying stage during sample preparation; therefore, the total analysis time is markedly reduced
compared with the combustion method. In addition, this newer approach is highly sensitive, so only small amounts of sample
are needed compared to the combustion method. However, despite these improved approaches and the significant interest in
75 the seasonal trends and source apportionment of WSOC, no studies have examined the change of $\delta^{13}\text{C}_{\text{WSOC}}$ in $\text{PM}_{2.5}$ over a
long period of time to understand seasonal variability. As mentioned above, the small particle size $\text{PM}_{2.5}$ contains large number
of WSOC, further investigations are needed. Here, we investigated the seasonal trends of WSOC at one suburban site and one
rural site in Japan. Samples of $\text{PM}_{2.5}$ were collected from July 2017 to July 2019 at both sites, and $\delta^{13}\text{C}_{\text{TC}}$ and $\delta^{13}\text{C}_{\text{WSOC}}$ values,
as well as carbon component and water-soluble ion concentrations, were determined. We then characterized the source of
WSOC and any atmospheric processes it had undergone using isotope-based approaches. We believe that this is the first report
80 of the use of the wet oxidation/IRMS method (Suto and Kawashima, 2018) for long-term observation of $\delta^{13}\text{C}_{\text{WSOC}}$.

2 Materials and experimental methods

2.1 Sampling sites and sample collection

Samples of $\text{PM}_{2.5}$ were collected at one suburban site and one rural site in Japan (Fig. S1 in the Supplement). The
suburban site (Tsukuba, 36°4'N, 140°4'E) was on the rooftop of a 25-m-high building at the Japan Automobile Research
85 Institute in Tsukuba City, Ibaraki Prefecture, Japan. Tsukuba is a suburban city located in the inland Kanto plain approximately
60 km northeast of the Tokyo metropolitan area. This site is surrounded by residential areas and forests, and there is a road in
front of the building. $\text{PM}_{2.5}$ samples were collected approximately every 10 days from 19 July 2017 to 12 July 2019. The rural
site (Yurihonjo, 39°23'N, 140°4'E) was on the campus of Akita Prefectural University in Yurihonjo City, Akita Prefecture,
Japan. Yurihonjo is located 370 km northwest of Tsukuba and about 5 km away from the coast. The sampling site had no local
90 pollutant sources such as large factories. Every year from December to February, the site is covered with several centimeters
of snow (Japan Meteorological, 2019). $\text{PM}_{2.5}$ samples were collected approximately every 14 days from 11 August 2017 to 5
July 2019.

At both sites, the $\text{PM}_{2.5}$ samples were collected with high-volume samplers (HV-1000F, Sibata Scientific
Technology, Saitama, Japan) equipped with a $\text{PM}_{2.5}$ impactor (HV-1000-PM_{2.5}, Sibata Scientific Technology) at a flow rate of
95 approximately 1000 L min⁻¹. The samples were collected on quartz fiber filters (20.3 × 25.4 cm, 2500QAT-UP, Pallflex,

Putnam, USA) that had been prebaked at 550 °C for 4 h before use. After sampling, the filters were kept in a freezer at –30 °C. A total of 107 PM_{2.5} samples (62 samples from Tsukuba and 45 samples from Yurihonjo) were collected. PM_{2.5} mass concentration was analyzed gravimetrically by using an electronic balance before and after sampling.

2.2 Stable carbon isotope ratio analysis

Determination of $\delta^{13}\text{C}_{\text{TC}}$ was performed at the Japan Automobile Research Institute using EA/IRMS (EA IsoLink, Thermo Fisher Scientific, Bremen, Germany; Delta V Advantage, Thermo Fisher Scientific, respectively). Portions of quartz filter (5–10 mg) were packed into a tin cup. The samples were combusted instantaneously with oxygen in the EA, and the carbon was converted to CO₂ via an oxidation/reduction tube of the EA. The oxidation/reduction tube and the packed column were maintained at 1020 °C and 60 °C, respectively. The flow rate of ultra-high-purity helium during the analysis was 180 mL min^{–1}. The CO₂ from the EA was ionized, and the $\delta^{13}\text{C}$ value was determined by means of IRMS; data acquisition was performed with Isodat software (ver. 3.0, Thermo Fisher Scientific).

Determination of $\delta^{13}\text{C}_{\text{wsoc}}$ was performed at Akita Prefectural University using the wet oxidation/IRMS method (Kawashima et al., 2018; Suto and Kawashima, 2018). A portion of each quartz fiber filter (14.13 cm²) was extracted in 5 mL of Milli-Q water under ultrasonic agitation for 30 min. The extract was filtered through a syringe filter (Chromatodisc Type A 0.45 µm, GL Sciences, Japan) to remove insoluble material. The PM_{2.5} samples were not decarbonated before $\delta^{13}\text{C}_{\text{wsoc}}$ analysis because the difference between the $\delta^{13}\text{C}_{\text{wsoc}}$ with and without hydrochloric acid pretreatment was within 0.2‰. A high-performance liquid chromatography (HPLC) system (Shimadzu Co.) was coupled to the IRMS instrument (Isoprime, Elementar UK, Manchester, UK) via a LiquiFace interface (Elementar UK). The HPLC system consisted of a column pump (LC-10ADvp), oxidation pump (LC-10ADvp), post-column pump (LC-10ADvp), autosampler (SIL-10ADvp), degasser (DGU-14A), and UV detector (SPD-10ADvp). The injection volume was 100 µL. The HPLC flow rate (without column), the sodium peroxodisulfate flow rate, and the post-column flow rate were 0.5, 0.4, and 0.3 mL min^{–1}, respectively. Sodium peroxodisulfate (0.5 M) and phosphoric acid (0.2 M) were mixed and then degassed in an ultrasonic bath for 1 h. One run took about 6 min. The trap current was set at 300 µA. The limits of detection (precision, $\leq\pm0.3\text{\%}$; accuracy, $\leq\pm0.3\text{\%}$) for levoglucosan and oxalic acid were 1111 and 1133 ngC, respectively.

The IRMS instrument and the data acquisition system were controlled by IonVantage NT software (ver. 1.5.4.0., Isoprime). The HPLC system was controlled by LCsolution software (ver. 1.25, Shimadzu Co.).

Stable carbon isotope ratios are expressed in δ notation in permil (‰)

$$\delta^{13}\text{C} [\text{\%}] = \left(\frac{R^{(13\text{C}/12\text{C})_{\text{sample}}}}{R^{(13\text{C}/12\text{C})_{\text{std}}}} - 1 \right) \quad (1)$$

where $R^{(13\text{C}/12\text{C})_{\text{sample}}}$ and $R^{(13\text{C}/12\text{C})_{\text{std}}}$ (= 0.0111802) are the $^{13}\text{C}/^{12}\text{C}$ ratios for the sample and the standard (Vienna Pee Dee Belemnite), respectively. For all samples, the EA/IRMS and wet oxidation/IRMS data were measured in triplicate.

A two-point linear calibration was carried out for $\delta^{13}\text{C}$ (Coplen et al., 2006). For EA/IRMS, $\delta^{13}\text{C}_{\text{TC}}$ values and three internal laboratory standards were calculated by using the following international isotopic standards: IAEA-CH-3 (cellulose, $\delta^{13}\text{C} = -24.724\text{\textperthousand}$), IAEA-600 (caffeine, $\delta^{13}\text{C} = -27.771\text{\textperthousand}$), and USGS24 (graphite, $\delta^{13}\text{C} = -16.049\text{\textperthousand}$). These standards were obtained from the International Atomic Energy Agency (Vienna, Austria). As a check of instrumental stability, an isotope 130 working standard (L-alanine, SI Science Co., Tokyo, Japan; $\delta^{13}\text{C} = -19.9\text{\textperthousand}$) was analyzed after every nine samples. For wet oxidation/IRMS, $\delta^{13}\text{C}$ values were calculated by means of a two-point linear calibration method from international isotope standards of sucrose (IAEA-CH-6, $\delta^{13}\text{C} = -10.449\text{\textperthousand}$), and three internal laboratory standards for D-(+)-arabitol ($\delta^{13}\text{C} = -23.6\text{\textperthousand}$), levoglucosan ($\delta^{13}\text{C} = -25.8\text{\textperthousand}$), and oxalic acid ($\delta^{13}\text{C} = -28.7\text{\textperthousand}$) obtained from EA/IRMS. Ultrapure water was prepared with a Milli-Q system (18.2 M $\Omega\text{.cm}$; Millipore, Bedford, MA). To check instrumental stability, the laboratory 135 standard of levoglucosan was analyzed after every nine samples. The average-1SD for $\delta^{13}\text{C}_{\text{TC}}$ and $\delta^{13}\text{C}_{\text{WSOC}}$ was 0.12 \textperthousand ($<0.46\text{\textperthousand}$) and 0.09 \textperthousand ($<0.50\text{\textperthousand}$), respectively, for all samples examined in the present study.

2.3 Chemical analysis

For determination of OC and EC concentrations, a portion of each quartz fiber filter (0.53 cm^2) was examined using a thermal-optical carbon analyzer (Model 2001, Desert Research Institute), and the samples were processed according to the 140 IMPROVE Thermal Desorption/Optical Reflectance method with a $550\text{ }^\circ\text{C}$, split for OC and EC (Chow et al., 2001). The limits of detection for OC and EC were determined as three times the standard deviation of a blank filter, and they were $0.02\text{ }\mu\text{g m}^{-3}$ and $0.02\text{ }\mu\text{g m}^{-3}$, respectively. These limits of detection were sufficiently low (Yamagami et al., 2019). For determination of WSOC concentrations, a portion of each quartz fiber filter (1.58 cm^2) was extracted with 8 mL of ultrapure 145 water for 30 min at room temperature. The water extracts were passed through a polyvinylidene difluoride filter (pore size $0.20\text{ }\mu\text{m}$, GE Healthcare, USA) to remove insoluble materials, and then the filtrate was analyzed using a total organic carbon analyzer (TOC-L, Shimadzu, Kyoto, Japan). The limit of detection was determined as three times the standard deviation of a blank filter, and it was $0.03\text{ }\mu\text{g m}^{-3}$, which was sufficiently low (Du et al., 2014). Quantification of the major water-soluble 150 ions anions (Cl^- , NO_2^- , NO_3^- , SO_4^{2-}) and cations (Na^+ , NH_4^+ , K^+ , Mg^{2+} , Ca^{2+}) was achieved by ion chromatography (Integriion RFIC; Thermo Fisher Scientific Inc., Sunnyvale, CA, USA). Details of water-soluble ion analysis method are described in Supplement S1.

3 Results and Discussion

3.1 Mass concentrations of $\text{PM}_{2.5}$ at the study sites

The average mass concentrations of $\text{PM}_{2.5}$ during the observation period were $19.7 \pm 8.2\text{ }\mu\text{g m}^{-3}$ (range, $7.1\text{--}46.6\text{ }\mu\text{g m}^{-3}$) in Tsukuba and $11.2 \pm 4.7\text{ }\mu\text{g m}^{-3}$ ($5.7\text{--}23.4\text{ }\mu\text{g m}^{-3}$) in Yurihonjo (Table 1). The average mass concentration of $\text{PM}_{2.5}$ in 155 Tsukuba was higher than the air quality standard for the annual average of Japan ($15\text{ }\mu\text{g m}^{-3}$) by the Ministry of the Environment and that at other residential sites across Japan (annual average in 2018, $11.2\text{ }\mu\text{g m}^{-3}$) (Ministry of the Environment,

2019). In Yurihonjo, the average mass concentration of $\text{PM}_{2.5}$ was lower than the air quality standard for the annual average of Japan, and it was comparable with that at other residential sites across Japan.

A previous study reviewed the annual $\text{PM}_{2.5}$ concentrations in 45 global megacities in 2013 (Cheng et al., 2016). The five most-polluted megacities were Delhi, India; Cairo, Egypt; and Xi'an, Tianjin, and Chengdu, China ($\text{PM}_{2.5}$ annual average concentration, $89\text{--}143 \mu\text{g m}^{-3}$). The five least-polluted megacities were Toronto, Canada; Miami, Philadelphia, and New York, United States; and Madrid, Spain ($\text{PM}_{2.5}$ annual average concentration, $7\text{--}10 \mu\text{g m}^{-3}$). The mass concentration of $\text{PM}_{2.5}$ at both sites in the present study was much closer to that determined for the least-polluted megacities than that determined for the most-polluted megacities. The mass concentrations of $\text{PM}_{2.5}$ in Tsukuba and Yurihonjo were significantly higher in winter and spring than in summer and autumn ($p < 0.01$). The mass concentrations of $\text{PM}_{2.5}$ were consistent with the seasonal variation for nearby sites of Atmospheric Environmental Regional Observation System (AEROS) provided by the Ministry of the Environment (Ministry of the Environment, 2021).

3.2 Concentrations of EC, OC, and WSOC, and OC/EC and WSOC/OC ratios

The concentrations of EC, OC, and WSOC, and the OC/EC and WSOC/OC ratios, at the study sites are summarized in Table 1. The concentrations of the carbon components (EC, WIOC, and WSOC) by season are shown in Fig. 1. The sum of EC and organic matter ($1.6 \times \text{OC}$ concentration) (Turpin and Lim, 2001) accounted for an average of 32% of the $\text{PM}_{2.5}$ mass concentration in Tsukuba and 25% in Yurihonjo. Thus, the contribution was slightly higher at Tsukuba than at Yurihonjo. The average EC concentration during the observation period was $0.9 \pm 0.4 \mu\text{g m}^{-3}$ ($0.4\text{--}2.4 \mu\text{g m}^{-3}$) in Tsukuba and $0.3 \pm 0.1 \mu\text{g m}^{-3}$ ($0.2\text{--}0.6 \mu\text{g m}^{-3}$) in Yurihonjo. These values are comparable to those reported for Nagoya ($1.1 \mu\text{g m}^{-3}$) (Yamagami et al., 2019) and Niigata ($0.5 \mu\text{g m}^{-3}$) (Li et al., 2018), Japan, and lower than that reported for Xi'an, China ($7.6 \mu\text{g m}^{-3}$) (Zhao et al., 2018). The EC concentration contributed an average of 5% to the $\text{PM}_{2.5}$ mass concentration in Tsukuba and 3% in Yurihonjo. Currently, EC concentrations in Japan are decreasing as a result of Japanese government regulations on emissions from diesel vehicles (Yamagami et al., 2019). The average OC concentration during the observation period was $3.2 \pm 1.4 \mu\text{g m}^{-3}$ ($1.0\text{--}6.6 \mu\text{g m}^{-3}$) in Tsukuba and $1.5 \pm 0.8 \mu\text{g m}^{-3}$ ($0.6\text{--}4.2 \mu\text{g m}^{-3}$) in Yurihonjo. The OC concentration contributed an average of 28% to the $\text{PM}_{2.5}$ mass concentration in Tsukuba and 22% in Yurihonjo. The higher percentage contribution to the $\text{PM}_{2.5}$ mass concentration from OC than EC was in agreement with compared to other studies (Contribution of OC and EC concentration in $\text{PM}_{2.5}$ concentration: 20% and 6% in Korea) (Park and Cho, 2011).

The OC/EC ratio is an indicator of the source of carbonaceous particles (Chow et al., 1996). The average OC/EC ratio was 3.8 ± 1.4 in Tsukuba and 5.1 ± 1.9 in Yurihonjo. The higher OC/EC ratio at the rural site (Yurihonjo) than at the suburban site (Tsukuba) was comparable with the results of other studies (Ho et al., 2006; Zhang et al., 2008). This was likely because primary emissions, such as EC, are low at rural sites, meaning that the OC is larger in comparison. The high OC/EC ratio is due to the formation of secondary organic aerosols and biomass burning (Chow et al., 1996).

The average WSOC concentration during the observation period was $1.2 \pm 0.4 \mu\text{g m}^{-3}$ ($0.4\text{--}2.4 \mu\text{g m}^{-3}$) in Tsukuba and $0.8 \pm 0.5 \mu\text{g m}^{-3}$ ($0.3\text{--}2.6 \mu\text{g m}^{-3}$) in Yurihonjo. These values were similar to those reported for Sapporo ($1.0 \mu\text{g m}^{-3}$)

190 (Pavuluri and Kawamura, 2017) and Maebashi (2.3 $\mu\text{g m}^{-3}$) (Kumagai et al., 2009), Japan, but lower than those reported for Beijing, China (7.2 $\mu\text{g m}^{-3}$) (Du et al., 2014), and Gwangju, South Korea (3.7 $\mu\text{g m}^{-3}$) (Park and Cho, 2011). The WSOC concentration at Tsukuba was significantly higher in autumn and winter than in spring and summer ($p < 0.01$), whereas that in Yurihonjo was significantly higher in spring than in the other seasons ($p < 0.05$). The average WSOC/OC ratio was 0.4 ± 0.1 in Tsukuba and 0.5 ± 0.1 in Yurihonjo. This is consistent with previous studies that showed that the average WSOC/OC ratio 195 was higher at rural sites than at urban sites (Kumagai et al., 2009; Ram and Sarin, 2010). This is also the same as the trend we found for OC/EC ratio in the present study.

3.3 $\delta^{13}\text{C}_{\text{TC}}$ and $\delta^{13}\text{C}_{\text{WSOC}}$

To our knowledge, this is the first report of a two-year-long observation of $\delta^{13}\text{C}_{\text{TC}}$ and $\delta^{13}\text{C}_{\text{WSOC}}$ in $\text{PM}_{2.5}$ at two sites simultaneously. $\delta^{13}\text{C}_{\text{WSOC}}$ values reported from previous studies conducted at various sampling sites and examining various 200 particle sizes are summarized in Table S1. In the present study, the average $\delta^{13}\text{C}_{\text{TC}}$ was $-25.7 \pm 0.7\text{\textperthousand}$ (-26.9 to $-24.0\text{\textperthousand}$) in Tsukuba and $-24.7 \pm 1.6\text{\textperthousand}$ (-27.3 to $-20.4\text{\textperthousand}$) in Yurihonjo (Table 1 and Fig. 2). Previous studies have reported the average $\delta^{13}\text{C}_{\text{TC}}$ of TSP in Sapporo, Japan ($-24.8\text{\textperthousand} \pm 0.68\text{\textperthousand}$) (Pavuluri and Kawamura, 2017), and of $\text{PM}_{2.5}$ in Sanjiang Plain, China ($-24.2\text{\textperthousand}$) (Cao et al., 2016), and these values are comparable to our present values.

In the present study, the average $\delta^{13}\text{C}_{\text{WSOC}}$ was $-25.2 \pm 1.1\text{\textperthousand}$ (-26.7 to $-21.8\text{\textperthousand}$) in Tsukuba and $-24.6 \pm 2.4\text{\textperthousand}$ (-28.4 to $-19.8\text{\textperthousand}$) in Yurihonjo (Table 1 and Fig. 2). The $\delta^{13}\text{C}_{\text{WSOC}}$ of $\text{PM}_{2.5}$, which was the particle size examined in the present 205 study, was $-25.4\text{\textperthousand} \pm 1.0\text{\textperthousand}$ in Delhi, India (Dasari et al., 2019), and $-24.2\text{\textperthousand} \pm 0.6\text{\textperthousand}$ in Bhola, Bangladesh (Dasari et al., 2019), which are very close to our $\delta^{13}\text{C}_{\text{WSOC}}$ values. The $\delta^{13}\text{C}_{\text{WSOC}}$ of TSP was $-24.2\text{\textperthousand} \pm 1.59\text{\textperthousand}$ in Sapporo, Japan (Pavuluri and Kawamura, 2017), $-24.0\text{\textperthousand} \pm 1.5\text{\textperthousand}$ in Seoul, South Korea (Han et al., 2020), $-25.2\text{\textperthousand} \pm 0.2\text{\textperthousand}$ in Millbrook, USA (Wozniak et al., 2012a), and similar values were obtained for particles of different sizes. In these previous studies, most of the 210 average $\delta^{13}\text{C}_{\text{WSOC}}$ values were in the range of $-25\text{\textperthousand}$ to $-24\text{\textperthousand}$ regardless of particle size, although there were some heavy values such as those for Hanimaadhoo Island, Maldives ($-18.4\text{\textperthousand} \pm 0.5\text{\textperthousand}$), and Sinhagad, India ($-20.4\text{\textperthousand} \pm 0.5\text{\textperthousand}$) (Kirillova et al., 2013a).

3.4 Seasonal variations in $\delta^{13}\text{C}_{\text{TC}}$ and $\delta^{13}\text{C}_{\text{WSOC}}$ in $\text{PM}_{2.5}$

$\delta^{13}\text{C}_{\text{TC}}$ and $\delta^{13}\text{C}_{\text{WSOC}}$ at Tsukuba showed no other clear seasonal variation, but they became slightly heavy from 215 February to April 2019 (Fig. 2a). In contrast, the $\delta^{13}\text{C}_{\text{TC}}$ and $\delta^{13}\text{C}_{\text{WSOC}}$ at Yurihonjo were heavier from autumn to spring than in summer (Fig. 2b), and they showed a significant seasonal variation ($\delta^{13}\text{C}_{\text{TC}}$; $p < 0.01$, $\delta^{13}\text{C}_{\text{WSOC}}$; $p < 0.01$) compared to those in Tsukuba. In addition, $\delta^{13}\text{C}_{\text{WSOC}}$ became heavier from February to April 2019 as in Tsukuba. At both study sites, $\delta^{13}\text{C}_{\text{WSOC}}$ was usually heavier than $\delta^{13}\text{C}_{\text{TC}}$, but in summer $\delta^{13}\text{C}_{\text{WSOC}}$ was comparable to or lighter than $\delta^{13}\text{C}_{\text{TC}}$ (Tsukuba; $p < 0.01$, Yurihonjo; $p < 0.01$).

220 The seasonal trends of $\delta^{13}\text{C}_{\text{TC}}$ and $\delta^{13}\text{C}_{\text{WSOC}}$ observed in the present study were compared with those reported from previous long-term observations. No seasonal variation for $\delta^{13}\text{C}_{\text{WSOC}}$ in the suburban site, Tsukuba is comparable with that in

TSP in Seoul, South Korea, from March 2015 to January 2016 (Han et al., 2020). Similarly, clearly trend for heavier in winter than in summer for $\delta^{13}\text{C}_{\text{TC}}$ and $\delta^{13}\text{C}_{\text{WSOC}}$ in the rural site, Yurihonjo is comparable with that in TSP reported for Sapporo, Japan, from September 2009 to October 2010 (Pavuluri and Kawamura, 2017). In both Yurihonjo and Sapporo, it was observed that $\delta^{13}\text{C}_{\text{WSOC}}$ is usually heavier than $\delta^{13}\text{C}_{\text{TC}}$ and that this tendency is reversed in summer. Together, these findings imply that $\delta^{13}\text{C}_{\text{WSOC}}$ shows a weak seasonal trend in suburban or urban sites such as Tsukuba and Seoul, but a clear seasonal trend in rural sites such as Yurihonjo and Sapporo.

The variations (difference between maximum and minimum value) of $\delta^{13}\text{C}_{\text{TC}}$ and $\delta^{13}\text{C}_{\text{WSOC}}$ were 2.9‰ and 4.9‰ in Tsukuba and 7.0‰ and 8.6‰ in Yurihonjo, respectively. The variation of $\delta^{13}\text{C}_{\text{WSOC}}$ was larger than that of $\delta^{13}\text{C}_{\text{TC}}$ at both sites, with both variations larger in Yurihonjo. In previous studies, the variation of $\delta^{13}\text{C}_{\text{TC}}$ was reported as 2.5‰ in Sapporo (Pavuluri and Kawamura, 2017), and that of $\delta^{13}\text{C}_{\text{WSOC}}$ was reported as 5.5‰ in Sapporo (Pavuluri and Kawamura, 2017), and 6.5‰ in Seoul (Han et al., 2020). The variation of $\delta^{13}\text{C}_{\text{EC}}$ of $\text{PM}_{2.5}$ was only 1.6‰ in Japan (Kawashima and Haneishi, 2012) and 3.7‰ in China (Ni et al., 2018; Zhao et al., 2018). In the present study and these previous studies, the variation of $\delta^{13}\text{C}_{\text{WSOC}}$ was larger than that of $\delta^{13}\text{C}_{\text{EC}}$, regardless of sampling site. The reason for this is likely that $\delta^{13}\text{C}_{\text{WSOC}}$ is affected not only by the source characteristics but also by atmospheric processing. The reasons underlying the seasonal trend observed for $\delta^{13}\text{C}_{\text{WSOC}}$ are further discussed in Sections 3.5.1 and 3.5.2.

3.5 Determination of seasonal trends and sources of WSOC using $\delta^{13}\text{C}_{\text{WSOC}}$

3.5.1 Seasonal trends and sources of WSOC in Tsukuba

The WSOC concentration in Tsukuba was significantly higher in autumn and winter than in spring and summer ($p < 0.01$), and EC concentration showed a similar seasonal trend ($p < 0.01$) (Table 1). Correlation coefficients between WSOC concentration and $\delta^{13}\text{C}_{\text{WSOC}}$, EC concentration, and non-sea-salt potassium (nss- K^+) concentration by season are shown in Table 2. A weak correlation ($r = 0.18$) was found between WSOC concentration and $\delta^{13}\text{C}_{\text{WSOC}}$. In contrast, the correlation coefficient between WSOC concentrations and EC concentrations, which is a tracer of combustion (Bond et al., 2007), was high in all seasons (annual average, $r = 0.71$), suggesting that WSOC was affected by combustion (e.g., fossil fuel and/or biomass burning) at this suburban site. The nss- K^+ is a tracer of biomass burning that is calculated by using the equation $\text{nss-}\text{K}^+ = [\text{K}^+] - 0.0335 \times [\text{Na}^+]$, which excludes K^+ originating from seawater (Lai et al., 2007). Strong correlations were observed between WSOC concentration and nss- K^+ in every season (autumn, $r = 0.96$; winter, $r = 0.83$; spring, $r = 0.85$; summer $r = 0.77$; $p < 0.01$), which suggests that WSOC was affected by biomass burning. The dominant annual source for WSOC was consistent with that reported in Seoul by Han et al. (2020).

The average $\delta^{13}\text{C}_{\text{WSOC}}$ was -25.2 ± 1.1 ‰ in Tsukuba. Since the C3 and C4 plants have different metabolic pathways, the $\delta^{13}\text{C}$ values are -34 to -24 ‰ for C3 plants and -19 to -6 ‰ for C4 plants, respectively (Smith and Epstein, 1971). When C3 plants are burned in the laboratory, there is no significant $\delta^{13}\text{C}$ difference between the produced particles and original C3 plants (Turekian et al., 1998; Das et al., 2010). In contrast, the particles produced by burning the C4 plants were 3.5‰ lighter

than the original C4 plants (Turekian et al., 1998). Therefore, the $\delta^{13}\text{C}$ of C4 plants was estimated to be -22.5 to $-9.5\text{\textperthousand}$. In fact, the $\delta^{13}\text{C}$ from C3 plants and C4 plants burning were -34.7 to $-25.1\text{\textperthousand}$ and -19.3 to $-16.1\text{\textperthousand}$, respectively (Kawashima and Haneishi, 2012; Garbaras et al., 2015; Guo et al., 2016). Thus, the average $\delta^{13}\text{C}_{\text{WSOC}}$ at Tsukuba suggested that biomass burning of C3 plants might be a dominant source. The most productive crop in Japan is rice, followed by barley and wheat (Ministry of Agriculture Forestry and Fisheries, 2018). In Ibaraki Prefecture, where Tsukuba city is located, the crop acreage of rice was 68,400 ha, and the harvest was 358,400 tons in 2018, the largest in the Kanto Region (Ministry of Agriculture Forestry and Fisheries, 2018). According to a field investigation, Tomiyama et al. (2017) reported that the biomass burning type and season in Tsukuba were rice straw and rice hulls, and from September to October, respectively. Using radiocarbon analysis, which can distinguish between biogenic and anthropogenic sources, a higher proportion of OC in $\text{PM}_{2.5}$ observed in Tokyo, Japan in 2014 was reported to be biogenic from autumn to winter than in summer (Hoshi and Saito, 2020).

The main chemical component generated by the breakdown of cellulose by burning rice straw is levoglucosan, which can be used as a tracer of biomass burning (Simoneit et al., 1999). The $\delta^{13}\text{C}$ of levoglucosan emitted from burning rice straw, peanut stalk, mulberry stalk, China fir, Chinese red pine, Chinese guger tree, Chestnut such as C3 plants ranged from -26.05 to $-22.60\text{\textperthousand}$, especially from rice straw, which was $-24.26 \pm 0.09\text{\textperthousand}$ (Sang et al., 2012). The average $\delta^{13}\text{C}_{\text{WSOC}}$ in Tsukuba was very close to the $\delta^{13}\text{C}$ of levoglucosan from burning rice straw. However levoglucosan concentration accounts for only about 3.8% of the WSOC concentration in urban area of Japan (Kumagai et al., 2010), and was very low percentages. Thus, it is difficult to compare the source directly using only the $\delta^{13}\text{C}$ of levoglucosan. In the future research, it should be considered to investigate the $\delta^{13}\text{C}$ of individual components not only levoglucosan.

3.5.2 Seasonal trends and sources of WSOC in Yurihonjo

The correlation in Yurihonjo between WSOC concentrations and EC concentrations was highest in winter ($r = 0.87$, $p < 0.01$), followed by autumn ($r = 0.83$, $p < 0.01$) and spring ($r = 0.64$, $p < 0.05$), and lowest in summer ($r = 0.24$) (Table 2). This suggests that WSOC was affected by combustion at this rural site during autumn and spring. In addition, the correlation between nss- K^+ concentration and WSOC concentration was very high in autumn ($r = 0.93$), winter ($r = 0.99$), and spring ($r = 0.80$; all $p < 0.01$) but not in summer ($r = 0.40$). These strong correlations suggest that the WSOC concentration from autumn to spring at Yurihonjo was mainly related to combustion sources such as biomass burning. The average $\delta^{13}\text{C}_{\text{WSOC}}$ at Yurihonjo was $-23.9 \pm 2.1\text{\textperthousand}$ during autumn and spring, suggesting that biomass burning of C3 plants such as rice straw and rice hulls may be a dominant source as in Tsukuba. In Akita Prefecture, an area of Japan famous for its rice production, the crop acreage of rice was 87,700 ha, and the harvest was 491,100 tons in 2018 (Ministry of Agriculture Forestry and Fisheries, 2018). From February to April 2019, $\delta^{13}\text{C}_{\text{WSOC}}$ was the heaviest with increasing WSOC concentrations (average, $1.5 \pm 0.7 \mu\text{g m}^{-3}$; $-21.3 \pm 1.9\text{\textperthousand}$) (Fig. 1b and Fig. 2b). The moderate correlation between $\delta^{13}\text{C}_{\text{WSOC}}$ and WSOC concentration was observed ($r = 0.54$, $p = 0.27 > 0.1$). This $\delta^{13}\text{C}_{\text{WSOC}}$ value might be related to heavy $\delta^{13}\text{C}$ source such as C4 plants (e.g., corn and grass). Around the sampling site at Yurihonjo, there was no evidence of burning of C4 plants during this period. Northeast China is the largest producer of corn in China (MWCACP, 2019), and biomass burning is actively used for heating in winter (Chen et al., 2017).

In Figure S2 in the Supplement, the number of fire spots were observed from February to April 2019 (NASA, 2017). The air mass backward trajectories showed that air masses during this period at Yurihonjo were mainly derived from areas located northeast China (Fig. S3 in the Supplement). For other air model, Uranishi et al. (2020) concluded that biomass burning in 290 northeast China was transported in Akita prefecture regions of Japan in February and March 2019 from Community Multiscale Air Quality model results. For water-soluble ion data, the correlation between Na^+ and Cl^- concentration was highest from winter to spring 2019 ($r = 0.98, p < 0.01$), suggesting the influence of sea salt. Recently, aerosol photochemical aging during 295 long-range transport selectively enriches the ^{13}C content in organic aerosols, leading to heavier $\delta^{13}\text{C}$ values in the remaining aerosol (Kirillova et al., 2013b; Bosch et al., 2014; Dasari et al., 2019; Zhang et al., 2019). In a field study, the isotope fractionation values for $\delta^{13}\text{C}_{\text{WSOC}}$ were estimated to be enriched by 3‰–4‰ because of aging during transport (Kirillova et al., 2013a). We speculate that the heavier $\delta^{13}\text{C}_{\text{WSOC}}$ from February to April 2019 at Yurihonjo might be affected by C4 plant burning and/or aging during long-term transport.

The $\delta^{13}\text{C}_{\text{WSOC}}$ in summer was very light ($-27.4\text{\textperthousand}$) compared with the average value for the observation period. The 300 weak correlation between WSOC concentration and EC concentration in summer ($r = 0.24$; Table 2) suggests that WSOC concentration is affected by some non-combustion source. In general, the formation of WSOC involves atmospheric reactions such as the formation of SOA. SOA is formed by oxidation of anthropogenic and biogenic VOCs (Heo et al., 2013). For anthropogenic VOCs, aliphatic hydrocarbons (e.g., alkanes and alkenes) and aromatics (e.g., benzene, toluene, ethylbenzene, and xylene) emitted from solvent evaporation and vehicle emissions are important anthropogenic VOCs precursors of SOA (Chen et al., 2010). The $\delta^{13}\text{C}$ values for alkanes in tunnel, gas station, underground garage, and refinery samples were reported 305 to range from $-28.6 \pm 1.8\text{\textperthousand}$ to $-27.3 \pm 2.1\text{\textperthousand}$ (Rudolph et al., 2002). Toluene and xylene are the aliphatic hydrocarbons with the highest annual emissions in Japan (Japan Ministry of Economy Trade and Industry, 2020). The $\delta^{13}\text{C}$ of toluene and xylene for gas station and vehicle emissions are reported to range from $-27.7\text{\textperthousand}$ to $-23.8\text{\textperthousand}$ (Rudolph et al., 2002; Kawashima and Murakami, 2014). For example, as VOCs in the atmosphere are oxidized by photochemical oxidants, the $\delta^{13}\text{C}$ of residual 310 VOCs becomes heavier by isotopic fractionation (Rudolph et al., 2000; Anderson et al., 2004). In other words, secondary production tends lighter $\delta^{13}\text{C}$ of SOA in the atmosphere. Actually, the $\delta^{13}\text{C}$ of SOA particles formed by photooxidation of toluene was 3 to 6‰ lighter in laboratory-based experiment than that of the precursor toluene, varying systematically with the extent of the oxidation reaction (Irei et al., 2006; Irei et al., 2011). Assuming this isotope fractionation for toluene applies also 315 to all other potential components, the $\delta^{13}\text{C}$ of the VOCs emission source for Yurihonjo was calculated as approximately -24.4 to $-21.4\text{\textperthousand}$ by subtracting 3 to 6‰ from the average $\delta^{13}\text{C}_{\text{WSOC}}$ during summer in Yurihonjo ($-27.4\text{\textperthousand}$). This estimated $\delta^{13}\text{C}$ value of VOCs was heavier than those previously reported for anthropogenic VOCs. Therefore, the anthropogenic VOCs was 320 considered no dominant source of WSOC.

For biogenic VOCs, the biogenic VOCs include isoprene, monoterpenes, and sesquiterpenes released from vegetation, with isoprene producing the most SOA (Atkinson and Arey, 1998). The oxidation product of isoprene is 2-methyltetro, which is widely used as an organic tracer to evaluate the production of SOA from isoprene (Claeys et al., 2004). The average $\delta^{13}\text{C}$ of 320 2-methyltetro in aerosols was $-27.36\text{\textperthousand}$ (-28.23 to $-26.46\text{\textperthousand}$) in four forests in Sichuan Province, China (Li et al., 2019). The

325 $\delta^{13}\text{C}$ of 2-methyltetrol is close to the $\delta^{13}\text{C}_{\text{WSOC}}$ detected in summer in Yurihonjo, suggesting that the components produced by secondary reaction of biogenic VOCs have a strong influence during summer in Yurihonjo. In field study, Miyazaki et al. (2012) reported that the lightest values of $\delta^{13}\text{C}_{\text{WSOC}}$ (average $-25.6 \pm 0.7\text{\textperthousand}$) was observed in forests of northern Japan from June to September. They have concluded from the PMF results that biogenic SOA production (isoprene SOA and α -/ β -pinene) were the dominant source of WSOC in summer, which was consistent with the conclusions of this study. At the global scale, biogenic VOCs emissions are more than an order of magnitude higher than those of anthropogenic VOCs (Farina et al., 2010).

4 Conclusion

330 The WSOC concentration, $\delta^{13}\text{C}_{\text{TC}}$ and the $\delta^{13}\text{C}_{\text{WSOC}}$ of $\text{PM}_{2.5}$ were observed at one suburban and one rural, in Japan over a two-year period. The average WSOC concentration during the observation period was $1.2 \pm 0.4 \text{ }\mu\text{g m}^{-3}$ (0.4 – $2.4 \text{ }\mu\text{g m}^{-3}$) in suburban site and $0.8 \pm 0.5 \text{ }\mu\text{g m}^{-3}$ (0.3 – $2.6 \text{ }\mu\text{g m}^{-3}$) in rural site. The $\delta^{13}\text{C}_{\text{WSOC}}$ was $-25.2 \pm 1.1\text{\textperthousand}$ (-26.7 to $-21.8\text{\textperthousand}$) in suburban site and $-24.6 \pm 2.4\text{\textperthousand}$ (-28.4 to $-19.8\text{\textperthousand}$) in rural site. The $\delta^{13}\text{C}_{\text{TC}}$ and $\delta^{13}\text{C}_{\text{WSOC}}$ at suburban site showed no other clear seasonal variation, but they became slightly heavy from February to April 2019. In contrast, the $\delta^{13}\text{C}_{\text{TC}}$ and $\delta^{13}\text{C}_{\text{WSOC}}$ at rural site were heavier from autumn to spring than in summer, and they showed a significant seasonal variation ($\delta^{13}\text{C}_{\text{TC}}$; $p < 0.01$, $\delta^{13}\text{C}_{\text{WSOC}}$; $p < 0.01$). By $\delta^{13}\text{C}_{\text{WSOC}}$, carbon components and water-soluble ions, at the suburban site, the main source of 335 WSOC was estimated biomass burning of rice straw. At the rural site, the $\delta^{13}\text{C}_{\text{WSOC}}$ from autumn to spring were a result mainly of biomass burning of rice straw, whereas the $\delta^{13}\text{C}_{\text{WSOC}}$ in summer was a result mainly of the formation of secondary organic aerosols from biogenic volatile organic compounds. In particular, the reason for the heaviest $\delta^{13}\text{C}_{\text{WSOC}}$ ($-21.3 \pm 1.9\text{\textperthousand}$) from February to April 2019 might be affected by long-range transport of C4 plant burning such as corn from overseas. Thus, we were able to use a $\delta^{13}\text{C}_{\text{WSOC}}$ based approach to understand the source characteristics of WSOC and the atmospheric processes 340 that contribute to the WSOC concentrations at the two study sites.

Data availability. Data are available from the corresponding author on request (nsuto@jari.or.jp).

345 **Author contribution.** NS and HK were involved in research planning and experimental design. NS performed the sampling and measurements of $\delta^{13}\text{C}_{\text{TC}}$, carbon components and water-soluble ions. HK performed the sampling and measurements of $\delta^{13}\text{C}_{\text{WSOC}}$. All authors clarified the experimental data and contributed to the writing of the paper.

Competing interests. The authors declare that they have no conflict of interest.

Acknowledgement

This work was partially supported by the Japan Society for the Promotion of Science KAKENHI Grant Numbers 355 19K20463, 18H03393, 17K12829, and 16KK0015. We acknowledge the use of data and imagery from NASA's Fire Information for Resource Management System (FIRMS) (<https://earthdata.nasa.gov/firms>), part of NASA's Earth Observing System Data and Information System (EOSDIS). We thank emeritus professor Shigeki Masunaga of Yokohama National University for providing the high-volume samplers used in this research, and Sae Ono, Momoka Suto, and Otoha Yoshida for collecting the aerosol samples and for helping wet oxidation/IRMS analysis at Akita Prefectural University. Furthermore, Dr. 360 Akiyoshi Ito, Dr. Hiroyuki Hagino, Kazue Kagami and Akemi Nakayama at Japan Automobile Research Institute, for their advice and help with chemical analysis. And, Yumi Sone from Thermo Fisher Scientific Inc., Japan was very helpful with our EA/IRMS analysis. Finally, we thank from ELSS, Inc. for editing the English of this manuscript.

References

365 Anderson, R. S., Iannone, R., Thompson, A. E., Rudolph, J., and Huang, L.: Carbon kinetic isotope effects in the gas-phase reactions of aromatic hydrocarbons with the OH radical at 296 ± 4 K, *Geophys. Res. Lett.*, 31, L15108, <https://10.1029/2004GL020089>, 2004.

Asa-Awuku, A., Moore, R. H., Nenes, A., Bahreini, R., Holloway, J. S., Brock, C. A., Middlebrook, A. M., Ryerson, T. B., Jimenez, J. L., DeCarlo, P. F., Hecobian, A., Weber, R. J., Stickel, R., Tanner, D. J., and Huey, L. G.: Airborne cloud condensation nuclei measurements during the 2006 Texas Air Quality Study, *J. Geophys. Res.*, 116, D11201, <https://10.1029/2010jd014874>, 2011.

Atkinson, R., and Arey, J.: Atmospheric Chemistry of Biogenic Organic Compounds, *Acc. Chem. Res.*, 31, 574-583, <https://10.1021/ar970143z>, 1998.

Bond, T. C., Bhardwaj, E., Dong, R., Jogani, R., Jung, S., Roden, C., Streets, D. G., and Trautmann, N. M.: Historical emissions 375 of black and organic carbon aerosol from energy-related combustion, 1850-2000, *Global Biogeochem. Cy.*, 21, GB2018, <https://10.1029/2006gb002840>, 2007.

Bosch, C., Andersson, A., Kirillova, E. N., Budhavant, K., Tiwari, S., Praveen, P. S., Russell, L. M., Beres, N. D., Ramanathan, V., and Gustafsson, Ö.: Source-diagnostic dual-isotope composition and optical properties of water-soluble organic carbon and elemental carbon in the South Asian outflow intercepted over the Indian Ocean, *J. Geophys. Res.*, 119, 380 11743-11759, <https://10.1002/2014JD022127>, 2014.

Cao, F., Zhang, S. C., Kawamura, K., and Zhang, Y. L.: Inorganic markers, carbonaceous components and stable carbon isotope from biomass burning aerosols in Northeast China, *Sci. Total Environ.*, 572, 1244-1251, <https://10.1016/j.scitotenv.2015.09.099>, 2016.

385 Cao, J. J., Chow, J. C., Tao, J., Lee, S. C., Watson, J. G., Ho, K. F., Wang, G. H., Zhu, C. S., and Han, Y. M.: Stable carbon isotopes in aerosols from Chinese cities: Influence of fossil fuels, *Atmos. Environ.*, 45, 1359-1363, <https://10.1016/j.atmosenv.2010.10.056>, 2011.

Chalbot, M. C. G., Brown, J., Chitranshi, P., Gamboa da Costa, G., Pollock, E. D., and Kavouras, I. G.: Functional characterization of the water-soluble organic carbon of size-fractionated aerosol in the southern Mississippi Valley, *Atmos. Chem. Phys.*, 14, 6075-6088, <https://10.5194/acp-14-6075-2014>, 2014.

390 Chen, J., Ying, Q., and Kleeman, M. J.: Source apportionment of wintertime secondary organic aerosol during the California regional PM₁₀/PM_{2.5} air quality study, *Atmos. Environ.*, 44, 1331-1340, <https://10.1016/j.atmosenv.2009.07.010>, 2010.

Chen, J., Li, C., Ristovski, Z., Milic, A., Gu, Y., Islam, M. S., Wang, S., Hao, J., Zhang, H., He, C., Guo, H., Fu, H., Miljevic, B., Morawska, L., Thai, P., Lam, Y. F., Pereira, G., Ding, A., Huang, X., and Dumka, U. C.: A review of biomass burning: Emissions and impacts on air quality, health and climate in China, *Sci. Total Environ.*, 579, 1000-1034, <https://10.1016/j.scitotenv.2016.11.025>, 2017.

395 Cheng, Z., Luo, L., Wang, S., Wang, Y., Sharma, S., Shimadera, H., Wang, X., Bressi, M., de Miranda, R. M., Jiang, J., Zhou, W., Fajardo, O., Yan, N., and Hao, J.: Status and characteristics of ambient PM_{2.5} pollution in global megacities, *Environ. Int.*, 89-90, 212-221, <https://10.1016/j.envint.2016.02.003>, 2016.

400 Chow, J. C., Watson, J. G., Lowenthal, D. H., Solomon, P. A., Magliano, K. L., Ziman, S. D., and Richards, L. W.: PM₁₀ and PM_{2.5} Compositions in California's San Joaquin Valley, *Aerosol Sci. Technol.*, 18, 105-128, <https://10.1080/02786829308959588>, 1993.

Chow, J. C., Watson, J. G., Lu, Z., Lowenthal, D. H., Frazier, C. A., Solomon, P. A., Thuillier, R. H., and Magliano, K.: Descriptive analysis of PM_{2.5} and PM₁₀ at regionally representative locations during SJVAQS/AUSPEX, *Atmos. Environ.*, 30, 2079-2112, [https://10.1016/1352-2310\(95\)00402-5](https://10.1016/1352-2310(95)00402-5), 1996.

405 Chow, J. C., Watson, J. G., Crow, D., Lowenthal, D. H., and Merrifield, T.: Comparison of IMPROVE and NIOSH Carbon Measurements, *Aerosol Sci. Technol.*, 34, 23-34, <https://10.1080/02786820119073>, 2001.

Claeys, M., Graham, B., Vas, G., Wang, W., Vermeylen, R., Pashynska, V., Cafmeyer, J., Guyon, P., Andreae, M. O., Artaxo, P., and Maenhaut, W.: Formation of secondary organic aerosols through photooxidation of isoprene, *Science*, 303, 1173-1176, <https://10.1126/science.1092805>, 2004.

410 Coplen, T. B., Brand, W. A., Gehre, M., Gröning, M., Meijer, H. A. J., Toman, B., and Verkouteren, R. M.: New Guidelines for $\delta^{13}\text{C}$ Measurements, *Anal. Chem.*, 78, 2439-2441, <https://10.1021/ac052027c>, 2006.

Das, O., Wang, Y., and Hsieh, Y.-P.: Chemical and carbon isotopic characteristics of ash and smoke derived from burning of C₃ and C₄ grasses, *Org. Geochem.*, 41, 263-269, <https://10.1016/j.orggeochem.2009.11.001>, 2010.

415 Dasari, S., Andersson, A., Bikkina, S., Holmstrand, H., Budhavant, K., Satheesh, S., Asmi, E., Kesti, J., Backman, J., Salam, A., Bisht, D. S., Tiwari, S., Hameed, Z., and Gustafsson, Ö.: Photochemical degradation affects the light absorption

of water-soluble brown carbon in the South Asian outflow, *Sci. Adv.*, 5, eaau8066, <https://10.1126/sciadv.aau8066>, 2019.

420 Decesari, S., Facchini, M. C., Matta, E., Lettini, F., Mircea, M., Fuzzi, S., Tagliavini, E., and Putaud, J. P.: Chemical features and seasonal variation of fine aerosol water-soluble organic compounds in the Po Valley, Italy, *Atmos. Environ.*, 35, 3691-3699, [https://10.1016/S1352-2310\(00\)00509-4](https://10.1016/S1352-2310(00)00509-4), 2001.

Du, Z., He, K., Cheng, Y., Duan, F., Ma, Y., Liu, J., Zhang, X., Zheng, M., and Weber, R.: A yearlong study of water-soluble organic carbon in Beijing I: Sources and its primary vs. secondary nature, *Atmos. Environ.*, 92, 514-521, <https://10.1016/j.atmosenv.2014.04.060>, 2014.

425 Duarte, R. M. B. O., Santos, E. B. H., Pio, C. A., and Duarte, A. C.: Comparison of structural features of water-soluble organic matter from atmospheric aerosols with those of aquatic humic substances, *Atmos. Environ.*, 41, 8100-8113, <https://10.1016/j.atmosenv.2007.06.034>, 2007.

Duarte, R. M. B. O., Freire, S. M. S. C., and Duarte, A. C.: Investigating the water-soluble organic functionality of urban aerosols using two-dimensional correlation of solid-state ^{13}C NMR and FTIR spectral data, *Atmos. Environ.*, 116, 245-252, <https://10.1016/j.atmosenv.2015.06.043>, 2015.

430 Farina, S. C., Adams, P. J., and Pandis, S. N.: Modeling global secondary organic aerosol formation and processing with the volatility basis set: Implications for anthropogenic secondary organic aerosol, *J. Geophys. Res.*, 115, D09202, <https://10.1029/2009jd013046>, 2010.

435 Fisseha, R., Saurer, M., Jäggi, M., Szidat, S., Siegwolf, R. T., and Baltensperger, U.: Determination of stable carbon isotopes of organic acids and carbonaceous aerosols in the atmosphere, *Rapid Commun. Mass Spectrom.*, 20, 2343-2347, <https://10.1002/rcm.2586>, 2006.

Fisseha, R., Saurer, M., Jäggi, M., Siegwolf, R. T. W., Dommen, J., Szidat, S., Samburova, V., and Baltensperger, U.: Determination of primary and secondary sources of organic acids and carbonaceous aerosols using stable carbon isotopes, *Atmos. Environ.*, 43, 431-437, <https://10.1016/j.atmosenv.2008.08.041>, 2009.

440 Garbaras, A., Masalaite, A., Garbariene, I., Ceburnis, D., Krugly, E., Remeikis, V., Puida, E., Kvietkus, K., and Martuzevicius, D.: Stable carbon fractionation in size-segregated aerosol particles produced by controlled biomass burning, *J. Aerosol Sci.*, 79, 86-96, <https://10.1016/j.jaerosci.2014.10.005>, 2015.

Gensch, I., Kiendler-Scharr, A., and Rudolph, J.: Isotope ratio studies of atmospheric organic compounds: Principles, methods, applications and potential, *Int. J. Mass spectrom.*, 365-366, 206-221, <https://10.1016/j.ijms.2014.02.004>, 2014.

445 Guo, Z., Jiang, W., Chen, S., Sun, D., Shi, L., Zeng, G., and Rui, M.: Stable isotopic compositions of elemental carbon in PM1.1 in north suburb of Nanjing Region, China, *Atmos. Res.*, 168, 105-111, <https://10.1016/j.atmosres.2015.09.006>, 2016.

Han, H., Kim, G., Seo, H., Shin, K.-H., and Lee, D.-H.: Significant seasonal changes in optical properties of brown carbon in the midlatitude atmosphere, *Atmos. Chem. Phys.*, 20, 2709-2718, <https://10.5194/acp-20-2709-2020>, 2020.

450 Heo, J., Dulger, M., Olson, M. R., McGinnis, J. E., Shelton, B. R., Matsunaga, A., Sioutas, C., and Schauer, J. J.: Source apportionments of PM_{2.5} organic carbon using molecular marker Positive Matrix Factorization and comparison of results from different receptor models, *Atmos. Environ.*, 73, 51-61, <https://10.1016/j.atmosenv.2013.03.004>, 2013.

Ho, K. F., Lee, S. C., Cao, J. J., Li, Y. S., Chow, J. C., Watson, J. G., and Fung, K.: Variability of organic and elemental carbon, water soluble organic carbon, and isotopes in Hong Kong, *Atmos. Chem. Phys.*, 6, 4569-4576, <https://10.5194/acp-6-4569-2006>, 2006.

455 Hoshi, J., and Saito, S.: Estimating the contribution of biomass burning to atmospheric organic particles at the central tokyo metropolitan area using levoglucosan and radiocarbon, *J. Jpn. Soc. Atmos. Environ.*, 55, 204-220, <https://10.11298/taiki.55.204>, 2020.

Irei, S., Huang, L., Collin, F., Zhang, W., Hastie, D., and Rudolph, J.: Flow reactor studies of the stable carbon isotope 460 composition of secondary particulate organic matter generated by OH-radical-induced reactions of toluene, *Atmos. Environ.*, 40, 5858-5867, <https://10.1016/j.atmosenv.2006.05.001>, 2006.

Irei, S., Rudolph, J., Huang, L., Auld, J., and Hastie, D.: Stable carbon isotope ratio of secondary particulate organic matter formed by photooxidation of toluene in indoor smog chamber, *Atmos. Environ.*, 45, 856-862, <https://10.1016/j.atmosenv.2010.11.021>, 2011.

465 Japan Meteorological Agency, Search for Past Climate Data 2017-2019: <http://www.jma.go.jp/jma/indexe.html>, access: 24 August, 2020.

Japan Ministry of Economy Trade and Industry, Pollutant Release and Transfer Register (PRTR): <http://www.env.go.jp/en/chemi/prtr/prtr.html>, access: 24 August, 2020.

Kawashima, H., and Haneishi, Y.: Effects of combustion emissions from the Eurasian continent in winter on seasonal $\delta^{13}\text{C}$ of 470 elemental carbon in aerosols in Japan, *Atmos. Environ.*, 46, 568-579, <https://10.1016/j.atmosenv.2011.05.015>, 2012.

Kawashima, H., and Murakami, M.: Measurement of the stable carbon isotope ratio of atmospheric volatile organic compounds using chromatography, combustion, and isotope ratio mass spectrometry coupled with thermal desorption, *Atmos. Environ.*, 89, 140-147, <https://10.1016/j.atmosenv.2014.02.033>, 2014.

Kawashima, H., Suto, M., and Suto, N.: Determination of carbon isotope ratios for honey samples by means of a liquid 475 chromatography/isotope ratio mass spectrometry system coupled with a post-column pump, *Rapid Commun. Mass Spectrom.*, 32, 1271-1279, <https://10.1002/rcm.8170>, 2018.

Kirillova, E. N., Sheesley, R. J., Andersson, A., and Gustafsson, Ö.: Natural Abundance ^{13}C and ^{14}C Analysis of Water-Soluble Organic Carbon in Atmospheric Aerosols, *Anal. Chem.*, 82, 7973-7978, <https://10.1021/ac1014436>, 2010.

Kirillova, E. N., Andersson, A., Sheesley, R. J., Kruså, M., Praveen, P. S., Budhavant, K., Safai, P. D., Rao, P. S. P., and 480 Gustafsson, Ö.: ^{13}C - and ^{14}C -based study of sources and atmospheric processing of water-soluble organic carbon (WSOC) in South Asian aerosols, *J. Geophys. Res.*, 118, 614-626, <https://10.1002/jgrd.50130>, 2013a.

Kirillova, E. N., Andersson, A., Sheesley, R. J., Kruså, M., Praveen, P. S., Budhavant, K., Safai, P. D., Rao, P. S. P., and Gustafsson, Ö.: ^{13}C - and ^{14}C -based study of sources and atmospheric processing of water-soluble organic carbon (WSOC) in South Asian aerosols, *J. Geophys. Res.*, 118, 614-626, <https://10.1002/jgrd.50130>, 2013b.

485 Kirillova, E. N., Andersson, A., Han, J., Lee, M., and Gustafsson, Ö.: Sources and light absorption of water-soluble organic carbon aerosols in the outflow from northern China, *Atmos. Chem. Phys.*, 14, 1413-1422, <https://10.5194/acp-14-1413-2014>, 2014a.

Kirillova, E. N., Andersson, A., Tiwari, S., Srivastava, A. K., Bisht, D. S., and Gustafsson, Ö.: Water-soluble organic carbon aerosols during a full New Delhi winter: Isotope-based source apportionment and optical properties, *J. Geophys. Res.*, 490 119, 3476-3485, <https://10.1002/2013jd020041>, 2014b.

Koch, D., Bond, T. C., Streets, D., Unger, N., and van der Werf, G. R.: Global impacts of aerosols from particular source regions and sectors, *J. Geophys. Res.*, 112, D02205, <https://10.1029/2005jd007024>, 2007.

Kumagai, K., Iijima, A., Tago, H., Tomioka, A., Kozawa, K., and Sakamoto, K.: Seasonal characteristics of water-soluble organic carbon in atmospheric particles in the inland Kanto plain, Japan, *Atmos. Environ.*, 43, 3345-3351, 495 <https://10.1016/j.atmosenv.2009.04.008>, 2009.

Kumagai, K., Iijima, A., Shimoda, M., Saitoh, Y., Kozawa, K., Hagino, H., and Sakamoto, K.: Determination of Dicarboxylic Acids and Levoglucosan in Fine Particles in the Kanto Plain, Japan, for Source Apportionment of Organic Aerosols, *Aerosol Air Qual. Res.*, 10, 282-291, <https://10.4209/aaqr.2009.11.0075>, 2010.

Lai, S., Zou, S., Cao, J., Lee, S., and Ho, K.: Characterizing ionic species in $\text{PM}_{2.5}$ and PM_{10} in four Pearl River Delta cities, 500 South China, *J. Environ. Sci.*, 19, 939-947, [https://10.1016/s1001-0742\(07\)60155-7](https://10.1016/s1001-0742(07)60155-7), 2007.

Li, L., Zhou, Y., Bi, X., Deng, S., Wang, S., and Lu, M.: Determination of the stable carbon isotopic compositions of 2-methyltetrols for four forest areas in Southwest China: The implications for the $\delta^{13}\text{C}$ values of atmospheric isoprene and C_3/C_4 vegetation distribution, *Sci. Total Environ.*, 678, 780-792, <https://10.1016/j.scitotenv.2019.04.432>, 2019.

Li, P., Sato, K., Hasegawa, H., Huo, M., Minoura, H., Inomata, Y., Take, N., Yuba, A., Futami, M., Takahashi, T., and Kotake, 505 Y.: Chemical Characteristics and Source Apportionment of $\text{PM}_{2.5}$ and Long-Range Transport from Northeast Asia Continent to Niigata in Eastern Japan, *Aerosol Air Qual. Res.*, 18, 938-956, <https://10.4209/aaqr.2017.05.0181>, 2018.

Lohmann, U., and Feichter, J.: Global indirect aerosol effects: A review, *Atmos. Chem. Phys.*, 5, 715-737, <https://10.5194/acp-5-715-2005>, 2005.

Malm, W. C., Schichtel, B. A., Pitchford, M. L., Ashbaugh, L. L., and Eldred, R. A.: Spatial and monthly trends in speciated 510 fine particle concentration in the United States, *J. Geophys. Res.*, 109, D03306, <https://10.1029/2003jd003739>, 2004.

Ministry of Agriculture Forestry and Fisheries, Statistical Survey on Crops: <https://www.maff.go.jp/e/index.html>, access: August 24, 2020.

Ministry of the Environment, air quality standard for the annual average of Japan: <http://www.env.go.jp/kijun/taiki.html>, access: August 24, 2020.

515 Ministry of the Environment, Atmospheric Environmental Regional Observation System (AEROS):
<http://www.env.go.jp/kijun/taiki.html>, access: February 22, 2021.

Miyazaki, Y., Fu, P. Q., Kawamura, K., Mizoguchi, Y., and Yamanoi, K.: Seasonal variations of stable carbon isotopic composition and biogenic tracer compounds of water-soluble organic aerosols in a deciduous forest, *Atmos. Chem. Phys.*, 12, 1367-1376, <https://10.5194/acp-12-1367-2012>, 2012.

520 MWCACP, USDA Major World Crop Areas and Climate Profiles: https://ipad.fas.usda.gov/rssiws/al/global_cropprod.aspx, access: May 26, 2021.

NASA, Fire Information for Resource Management System (FIRMS): <https://earthdata.nasa.gov/firms>, access: May 26, 2021.

Ni, H., Huang, R. J., Cao, J., Liu, W., Zhang, T., Wang, M., Meijer, H. A. J., and Dusek, U.: Source apportionment of carbonaceous aerosols in Xi'an, China: insights from a full year of measurements of radiocarbon and the stable isotope 525 ^{13}C , *Atmos. Chem. Phys.*, 18, 16363-16383, <https://10.5194/acp-18-16363-2018>, 2018.

Padró, L. T., Tkacik, D., Lathem, T., Hennigan, C. J., Sullivan, A. P., Weber, R. J., Huey, L. G., and Nenes, A.: Investigation of cloud condensation nuclei properties and droplet growth kinetics of the water-soluble aerosol fraction in Mexico City, *J. Geophys. Res.*, 115, D09204, <https://10.1029/2009jd013195>, 2010.

Park, S. S., and Cho, S. Y.: Tracking sources and behaviors of water-soluble organic carbon in fine particulate matter measured 530 at an urban site in Korea, *Atmos. Environ.*, 45, 60-72, <https://10.1016/j.atmosenv.2010.09.045>, 2011.

Pavuluri, C. M., and Kawamura, K.: Seasonal changes in TC and WSOC and their ^{13}C isotope ratios in Northeast Asian aerosols: land surface–biosphere–atmosphere interactions, *Acta Geochim.*, 36, 355-358, <https://10.1007/s11631-017-0157-3>, 2017.

Pietrogrande, M. C., Bacco, D., and Chiereghin, S.: GC/MS analysis of water-soluble organics in atmospheric aerosol: 535 optimization of a solvent extraction procedure for simultaneous analysis of carboxylic acids and sugars, *Anal. Bioanal. Chem.*, 405, 1095-1104, <https://10.1007/s00216-012-6592-4>, 2013.

Pope, C. A., Thun, M. J., Namboodiri, M. M., Dockery, D. W., Evans, J. S., Speizer, F. E., and Heath Jr, C. W.: Particulate air pollution as a predictor of mortality in a prospective study of U.S. Adults, *Am. J. Respir. Crit. Care Med.*, 151, 669-674, https://10.1164/ajrccm/151.3_Pt_1.669, 1995.

540 Pöschl, U.: Atmospheric Aerosols: Composition, Transformation, Climate and Health Effects, *Angew. Chem. Int. Ed.*, 44, 7520-7540, <https://10.1002/anie.200501122>, 2005.

Ram, K., and Sarin, M. M.: Spatio-temporal variability in atmospheric abundances of EC, OC and WSOC over Northern India, *J. Aerosol Sci.*, 41, 88-98, <https://10.1016/j.jaerosci.2009.11.004>, 2010.

Rudolph, J., Czuba, E., and Huang, L.: The stable carbon isotope fractionation for reactions of selected hydrocarbons with 545 OH-radicals and its relevance for atmospheric chemistry, *J. Geophys. Res.*, 105, 29329-29346, <https://10.1029/2000JD900447>, 2000.

Rudolph, J., Czuba, E., Norman, A. L., Huang, L., and Ernst, D.: Stable carbon isotope composition of nonmethane hydrocarbons in emissions from transportation related sources and atmospheric observations in an urban atmosphere, *Atmos. Environ.*, 36, 1173-1181, [https://10.1016/S1352-2310\(01\)00537-4](https://10.1016/S1352-2310(01)00537-4), 2002.

550 Saarikoski, S., Timonen, H., Saarnio, K., Aurela, M., J̄rvi, L., Keronen, P., Kerminen, V. M., and Hillamo, R.: Sources of organic carbon in fine particulate matter in northern European urban air, *Atmos. Chem. Phys.*, 8, 6281-6295, <https://10.5194/acp-8-6281-2008>, 2008.

Sang, X. F., Gensch, I., Laumer, W., Kammer, B., Chan, C. Y., Engling, G., Wahner, A., Wissel, H., and Kiendler-Scharr, A.: Stable carbon isotope ratio analysis of anhydrosugars in biomass burning aerosol particles from source samples, 555 *Environ. Sci. Technol.*, 46, 3312-3318, <https://10.1021/es204094v>, 2012.

Schichtel, B. A., Malm, W. C., Bench, G., Fallon, S., McDade, C. E., Chow, J. C., and Watson, J. G.: Fossil and contemporary fine particulate carbon fractions at 12 rural and urban sites in the United States, *J. Geophys. Res.*, 113, D02311, <https://10.1029/2007jd008605>, 2008.

560 Simoneit, B. R. T., Schauer, J. J., Nolte, C. G., Oros, D. R., Elias, V. O., Fraser, M. P., Rogge, W. F., and Cass, G. R.: Levoglucosan, a tracer for cellulose in biomass burning and atmospheric particles, *Atmos. Environ.*, 33, 173-182, [https://10.1016/S1352-2310\(98\)00145-9](https://10.1016/S1352-2310(98)00145-9), 1999.

Smith, B. N., and Epstein, S.: Two Categories of $^{13}\text{C}/^{12}\text{C}$ Ratios for Higher Plants, *Plant Physiol.*, 47, 380-384, <https://10.1104/pp.47.3.380>, 1971.

Sullivan, A. P., Weber, R. J., Clements, A. L., Turner, J. R., Bae, M. S., and Schauer, J. J.: A method for on-line measurement 565 of water-soluble organic carbon in ambient aerosol particles: Results from an urban site, *Geophys. Res. Lett.*, 31, L13105, <https://10.1029/2004gl019681>, 2004.

Sullivan, A. P., and Weber, R. J.: Chemical characterization of the ambient organic aerosol soluble in water: 2. Isolation of acid, neutral, and basic fractions by modified size-exclusion chromatography, *J. Geophys. Res.*, 111, D05315, <https://10.1029/2005jd006486>, 2006.

570 Suto, N., and Kawashima, H.: Online wet oxidation/isotope ratio mass spectrometry method for determination of stable carbon isotope ratios of water-soluble organic carbon in particulate matter, *Rapid Commun. Mass Spectrom.*, 32, 1668-1674, <https://10.1002/rcm.8240>, 2018.

Timonen, H., Carbone, S., Aurela, M., Saarnio, K., Saarikoski, S., Ng, N. L., Canagaratna, M. R., Kulmala, M., Kerminen, V.-M., Worsnop, D. R., and Hillamo, R.: Characteristics, sources and water-solubility of ambient submicron organic 575 aerosol in springtime in Helsinki, Finland, *J. Aerosol Sci.*, 56, 61-77, <https://10.1016/j.jaerosci.2012.06.005>, 2013.

Tomiyama, H., Tanabe, K., Chatani, S., Kobayashi, S., Fujitani, Y., Furuyama, A., Sato, K., Fushimi, A., Kondo, Y., Sugata, S., Morino, Y., Hayasaki, M., Oguma, H., Ide, R., Kusaka, H., and Takami, A.: Observation for Temporal Open Burning Frequency and Estimation for Daily Emissions caused by Open Burning of Rice Residue, *J. Jpn. Soc. Atmos. Environ.*, 52, 105-117, <https://10.11298/taiki.52.105>, 2017.

580 Turekian, V. C., Macko, S., Ballentine, D., Swap, R. J., and Garstang, M.: Causes of bulk carbon and nitrogen isotopic fractionations in the products of vegetation burns: laboratory studies, *Chem. Geol.*, 152, 181-192, [https://10.1016/S0009-2541\(98\)00105-3](https://10.1016/S0009-2541(98)00105-3), 1998.

Turpin, B. J., and Lim, H.-J.: Species Contributions to PM_{2.5} Mass Concentrations: Revisiting Common Assumptions for Estimating Organic Mass, *Aerosol Sci. Technol.*, 35, 602-610, <https://10.1080/02786820119445>, 2001.

585 Uranishi, K., Ikemori, F., Shimadera, H., Kondo, A., and Sugata, S.: Air Quality Simulation of PM_{2.5} Transboundary Pollution over Northeast Asia Caused by Biomass Burning in Northeast China: A Case Study in Hokkaido, Japan, in Early Spring of 2019, *J. Jpn. Soc. Atmos. Environ.*, 55, 34-49, <https://10.11298/taiki.55.34>, 2020.

590 Widory, D., Roy, S., Le Moullec, Y., Goupil, G., Cocherie, A., and Guerrot, C.: The origin of atmospheric particles in Paris: a view through carbon and lead isotopes, *Atmos. Environ.*, 38, 953-961, <https://10.1016/j.atmosenv.2003.11.001>, 2004.

Wozniak, A. S., Bauer, J. E., and Dickhut, R. M.: Characteristics of water-soluble organic carbon associated with aerosol particles in the eastern United States, *Atmos. Environ.*, 46, 181-188, <https://10.1016/j.atmosenv.2011.10.001>, 2012a.

Wozniak, A. S., Bauer, J. E., Dickhut, R. M., Xu, L., and McNichol, A. P.: Isotopic characterization of aerosol organic carbon components over the eastern United States, *J. Geophys. Res.*, 117, D13303, <https://10.1029/2011JD017153>, 2012b.

595 Yamagami, M., Ikemori, F., Nakashima, H., Hisatsune, K., and Osada, K.: Decreasing trend of elemental carbon concentration with changes in major sources at Mega city Nagoya, Central Japan, *Atmos. Environ.*, 199, 155-163, <https://10.1016/j.atmosenv.2018.11.014>, 2019.

600 Yan, C., Zheng, M., Bosch, C., Andersson, A., Desyaterik, Y., Sullivan, A. P., Collett, J. L., Zhao, B., Wang, S., He, K., and Gustafsson, O.: Important fossil source contribution to brown carbon in Beijing during winter, *Sci. Rep.*, 7, 43182, <https://10.1038/srep43182>, 2017.

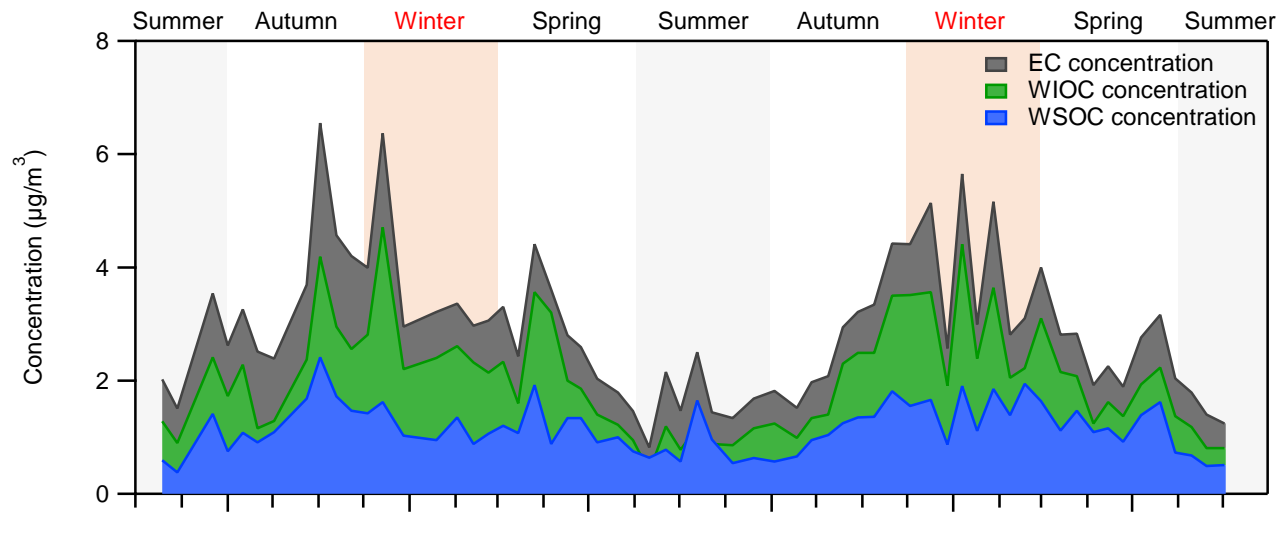
Yu, J. Z., Yang, H., Zhang, H., and Lau, A. K. H.: Size distributions of water-soluble organic carbon in ambient aerosols and its size-resolved thermal characteristics, *Atmos. Environ.*, 38, 1061-1071, <https://10.1016/j.atmosenv.2003.10.049>, 2004.

605 Zhang, W., Zhang, Y.-L., Cao, F., Xiang, Y., Zhang, Y., Bao, M., Liu, X., and Lin, Y.-C.: High time-resolved measurement of stable carbon isotope composition in water-soluble organic aerosols: method optimization and a case study during winter haze in eastern China, *Atmos. Chem. Phys.*, 19, 11071-11087, <https://10.5194/acp-19-11071-2019>, 2019.

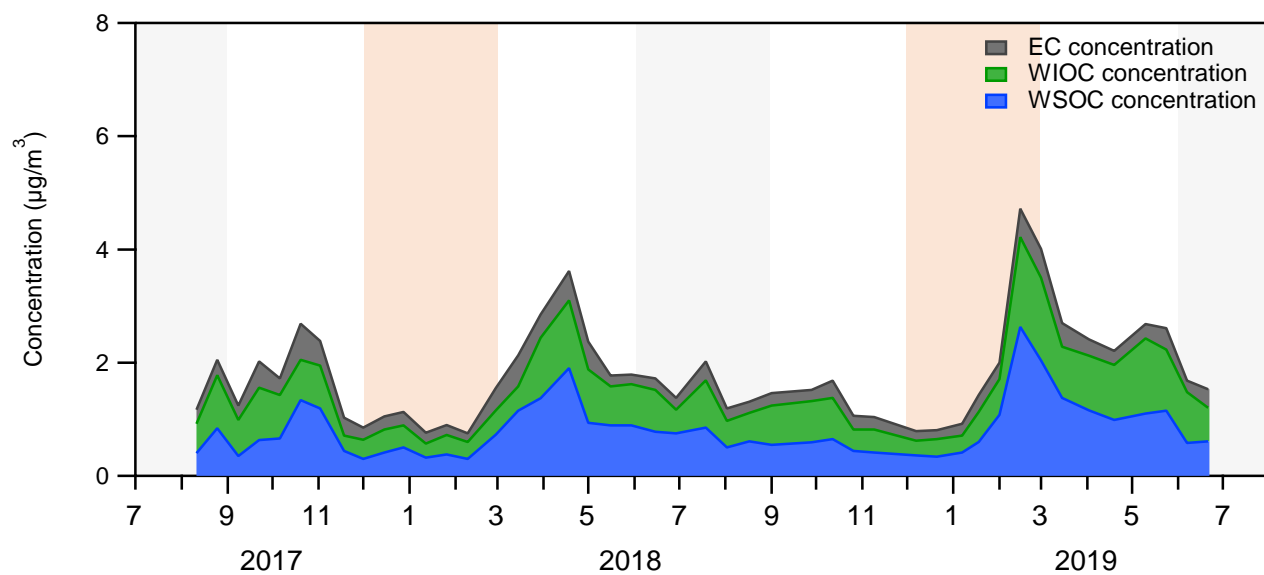
Zhang, X. Y., Wang, Y. Q., Zhang, X. C., Guo, W., and Gong, S. L.: Carbonaceous aerosol composition over various regions of China during 2006, *J. Geophys. Res.*, 113, D14111, <https://10.1029/2007jd009525>, 2008.

610 Zhao, Z., Cao, J., Zhang, T., Shen, Z., Ni, H., Tian, J., Wang, Q., Liu, S., Zhou, J., Gu, J., and Shen, G.: Stable carbon isotopes and levoglucosan for PM_{2.5} elemental carbon source apportionments in the largest city of Northwest China, *Atmos. Environ.*, 185, 253-261, <https://10.1016/j.atmosenv.2018.05.008>, 2018.

615 (a) Tsukuba, Ibaraki



620 (b) Yurihonjo, Akita



630 640 Figure 1: Concentrations of EC, WIOC, and WSOC of $\text{PM}_{2.5}$ from July 2017 to July 2019 in (a) Tsukuba, Ibaraki, and (b) Yurihonjo, Akita, Japan.

645

650 (a) Tsukuba, Ibaraki

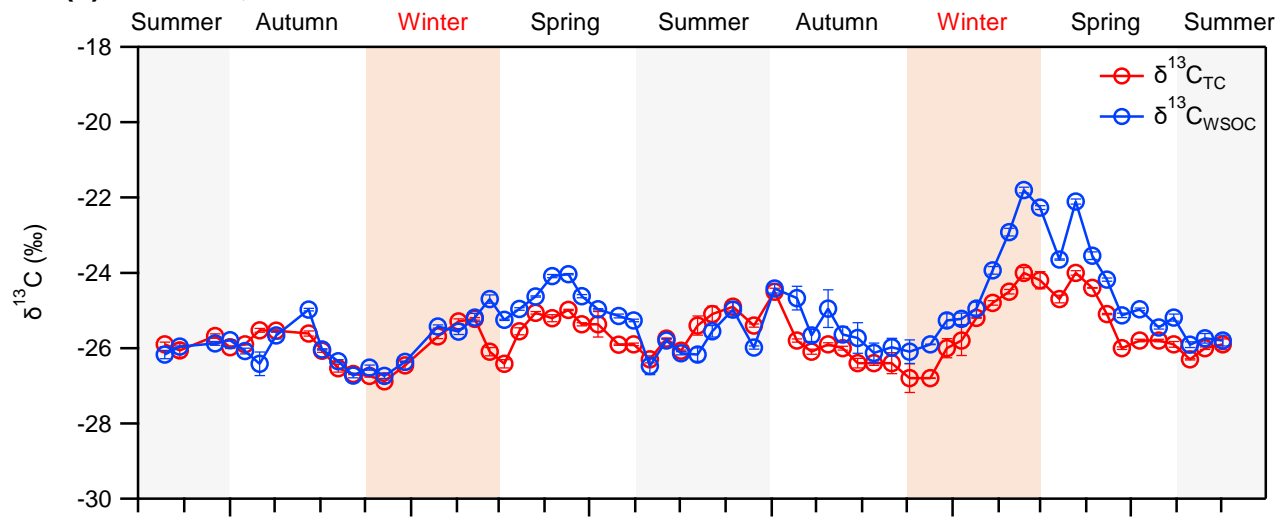


Table 1. Seasonal average concentrations of PM_{2.5}, EC, OC, and WSOC; OC/EC and WSOC/OC ratios; and $\delta^{13}\text{C}_{\text{TC}}$ and680 $\delta^{13}\text{C}_{\text{WSOC}}$ values for PM_{2.5} in Tsukuba and Yurihonjo, Japan.

Tsukuba

| Compound | Season (average \pm SD) | | | | Average (n = 62) |
|--|---------------------------|--------------------|--------------------|--------------------|---------------------|
| | Spring (n = 18) | Summer (n = 13) | Autumn (n = 16) | Winter (n = 15) | |
| PM _{2.5} ($\mu\text{g m}^{-3}$) | 23.5 \pm 7.7 | 14.4 \pm 4.1 | 16.5 \pm 7.2 | 23.0 \pm 8.9 | 19.7 \pm 8.2 |
| EC ($\mu\text{g m}^{-3}$) | 0.7 \pm 0.2 | 0.7 \pm 0.3 | 1.1 \pm 0.5 | 1.0 \pm 0.4 | 0.9 \pm 0.4 |
| OC ($\mu\text{g m}^{-3}$) | 3.2 \pm 1.0 | 1.8 \pm 0.8 | 3.4 \pm 1.4 | 4.2 \pm 1.2 | 3.2 \pm 1.4 |
| WSOC ($\mu\text{g m}^{-3}$) | 1.2 \pm 0.3 | 0.8 \pm 0.4 | 1.3 \pm 0.5 | 1.4 \pm 0.4 | 1.2 \pm 0.4 |
| OC/EC | 4.5 \pm 1.6 | 2.7 \pm 0.6 | 3.5 \pm 1.2 | 4.4 \pm 0.8 | 3.8 \pm 1.4 |
| WSOC/OC | 0.4 \pm 0.1 | 0.4 \pm 0.1 | 0.4 \pm 0.0 | 0.3 \pm 0.1 | 0.4 \pm 0.1 |
| $\delta^{13}\text{C}_{\text{TC}}$ (‰) | -25.3 \pm 0.7 | -25.8 \pm 0.4 | -26.0 \pm 0.5 | -25.7 \pm 0.9 | -25.7 \pm 0.7 |
| $\delta^{13}\text{C}_{\text{WSOC}}$ (‰) | -24.4 \pm 1.0 | -25.9 \pm 0.4 | -25.7 \pm 0.6 | -25.1 \pm 1.4 | -25.2 \pm 1.1 |

Yurihonjo

| Compound | Season (average \pm SD) | | | | Average (n = 45) |
|--|---------------------------|-------------------|--------------------|--------------------|---------------------|
| | Spring (n = 12) | Summer (n = 9) | Autumn (n = 11) | Winter (n = 13) | |
| PM _{2.5} ($\mu\text{g m}^{-3}$) | 15.8 \pm 4.2 | 8.6 \pm 2.4 | 8.1 \pm 1.2 | 11.4 \pm 5.1 | 11.2 \pm 4.7 |
| EC ($\mu\text{g m}^{-3}$) | 0.4 \pm 0.1 | 0.2 \pm 0.1 | 0.3 \pm 0.1 | 0.2 \pm 0.1 | 0.3 \pm 0.1 |
| OC ($\mu\text{g m}^{-3}$) | 2.2 \pm 0.6 | 1.3 \pm 0.3 | 1.3 \pm 0.5 | 1.1 \pm 1.0 | 1.5 \pm 0.8 |
| WSOC ($\mu\text{g m}^{-3}$) | 1.2 \pm 0.4 | 0.7 \pm 0.2 | 0.7 \pm 0.3 | 0.6 \pm 0.6 | 0.8 \pm 0.5 |
| OC/EC | 6.6 \pm 2.1 | 5.5 \pm 1.5 | 4.2 \pm 1.2 | 4.1 \pm 1.5 | 5.1 \pm 1.9 |
| WSOC/OC | 0.6 \pm 0.1 | 0.5 \pm 0.1 | 0.5 \pm 0.1 | 0.6 \pm 0.1 | 0.5 \pm 0.1 |
| $\delta^{13}\text{C}_{\text{TC}}$ (‰) | -24.4 \pm 1.6 | -26.2 \pm 0.7 | -25.3 \pm 1.3 | -23.5 \pm 1.2 | -24.7 \pm 1.6 |
| $\delta^{13}\text{C}_{\text{WSOC}}$ (‰) | -23.8 \pm 2.0 | -27.4 \pm 0.7 | -25.5 \pm 2.0 | -22.6 \pm 1.3 | -24.6 \pm 2.4 |

685

690

Table 2. Correlation (r) between WSOC concentration and the stated parameters.

695

| Season | Tsukuba | | | Yurihonjo | | |
|--------|-------------------------------------|------|--------------------|-------------------------------------|------|--------------------|
| | $\delta^{13}\text{C}_{\text{WSOC}}$ | EC | nss-K ⁺ | $\delta^{13}\text{C}_{\text{WSOC}}$ | EC | nss-K ⁺ |
| Spring | 0.36 | 0.73 | 0.85 | 0.63 | 0.64 | 0.80 |
| Summer | -0.14 | 0.84 | 0.77 | 0.17 | 0.24 | 0.40 |
| Autumn | -0.45 | 0.75 | 0.96 | 0.65 | 0.83 | 0.93 |
| Winter | 0.29 | 0.68 | 0.83 | 0.77 | 0.87 | 0.99 |
| Annual | 0.18 | 0.71 | 0.88 | 0.44 | 0.72 | 0.87 |